Field Study Of Transit Time Through Compacted Clays

Interim Annual Report

July 1, 1989 to June 30, 1990

For

Contract No. SENR-HWR-90-47

Keros Cartwright, Principal Investigator

Project Manager:
Ivan G. Krapac

Project Participants:
Samuel Panno
Beverly Herzog
Bruce Hensel
Kenneth Rehfeldt

Open File Series 1990-11

Illinois State Geological Survey
Champaign, Illinois

Prepared for

Dr. Gary Miller
Hazardous Waste Research and Information Center
1808 Woodfield Drive
Savoy, Illinois 61874

Table of Contents

Introduction

Despite an increased emphasis on recycling, waste reduction, and waste-to-energy conversion for the alleviation of the waste disposal crisis, land burial of solid wastes will continue to be an integral part of any waste management plan (Birks, 1989). In land burial schemes, compacted soil barriers with low hydraulic conductivity are commonly used in cover and liner systems to control the movement of liquids and prevent groundwater contamination. Little research has been done to evaluate the effectiveness of field-scale compacted soil barriers in retarding the movement of water and leachates. In response to this need, the Illinois Hazardous Waste Research and Information Center began support, in 1987, of a soil liner research program being conducted at the Illinois State Geological Survey. In particular, project number SENR-HWR-90-047 entitled, "Field Study Of Transit Time Through Compacted Clays" has provided support for the second year of monitoring a field- scale soil liner.

This report summarizes the data collected and analyzed during the period May 1, 1989 to June 30, 1990 and compares these results with those collected during the first year of liner monitoring (April 1988 to April 1989). The objectives of this study were: 1) to determine the saturated hydraulic conductivity of a soil liner, 2) to evaluate if the hydraulic conductivity was less than 1×10^{-7} cm/s as required by the U.S. EPA, 3) to determine the spatial variability of liner hydraulic properties, and 4) to measure and predict water and tracer movement through a soil liner.

Methods

Ring infiltrometers were used to measure the rate of infiltration of water into the liner as a basis for calculating saturated hydraulic conductivity (K_{sat}). Ideally, the initiation of ponding of a soil or liner results in a rate of infiltration that is relatively high and is dominated by a matric potential gradient. As the matric gradient decreases, the infiltration flux[1] asymptotically decreases with time until a constant gravity-induced infiltration flux is approached. A constant rate of infiltration signifies the achievement of steady-state

[1]The term "infiltration flux" is defined as the volume of water that infiltrated over a specific period of time (cm/s) into a specific areal extent of the liner. Infiltration flux divided by the hydraulic gradient is equal to saturated hydraulic conductivity (K_{sat}).

infiltrability (defined by Hillel, 1982) that is dominated by gravity and is directly proportional to the K_{sat} and hydraulic gradient. The hydraulic gradient of the liner was determined experimentally from tensiometer data; lateral flow of infiltrating water was assumed to be negligible because of the experimental design of the liner.

Four large-ring (LR) and thirty-two small-ring (SR) infiltrometers (1.5 m and 0.3 m OD, respectively) were installed into the liner. These instruments provided replication of infiltration fluxes between liner quadrants and a means to study spatial dependence of K_{sat} throughout the liner (Fig. 1a). The number and location of infiltrometers were determined using classical statistical and geostatistical estimates of optimal sample numbers, and based on work by Rogowski et al. (1985). The LR infiltrometers were installed in accordance with procedures developed by Daniel (1984). The SR infiltrometers were installed and modified from the design used by Rogowski (1989) such that infiltration flux could be measured by the same techniques used in the LR-infiltrometers (Fig. 1b).

The difference in the size of the infiltrometers represents two scales of measurement for infiltration. A third scale used to estimate the infiltration flux of the liner utilized a water-balance of the entire liner. For this latter calculation, the volume of water which evaporated from the pond (based on water loss from evaporation pans) was subtracted from the amount of water required to maintain a constant pond level.

For each infiltration ring and for the entire liner, cumulative-infiltration volumes were plotted and regressed with respect to time. The slope of the regression equation divided by the cross-sectional area of each infiltrometer represented the "average" steady-state infiltrability or infiltration flux. The K_{sat} for all three scales was calculated using the infiltration flux and measured hydraulic gradient.

Tritiated water was added to the liner pond to monitor water movement through the liner and to identify the effect of diffusion as a mechanism for the movement of contaminants through compacted soil barriers. Pond and soil water samples were collected monthly and quarterly, respectively. As many as 17 locations in the pond were sampled to obtain an "average" tritium concentration for the pond. Soil water samples were collected at six depths (10, 18, 33, 51, 69, 89 cm) in the liner using suction vacuum lysimeters (see Krapac et al., 1989a for locations and sampling procedures). All samples were analyzed for tritium using a Packard Tri-Carb 2000 Liquid Scintillation Analyzer.

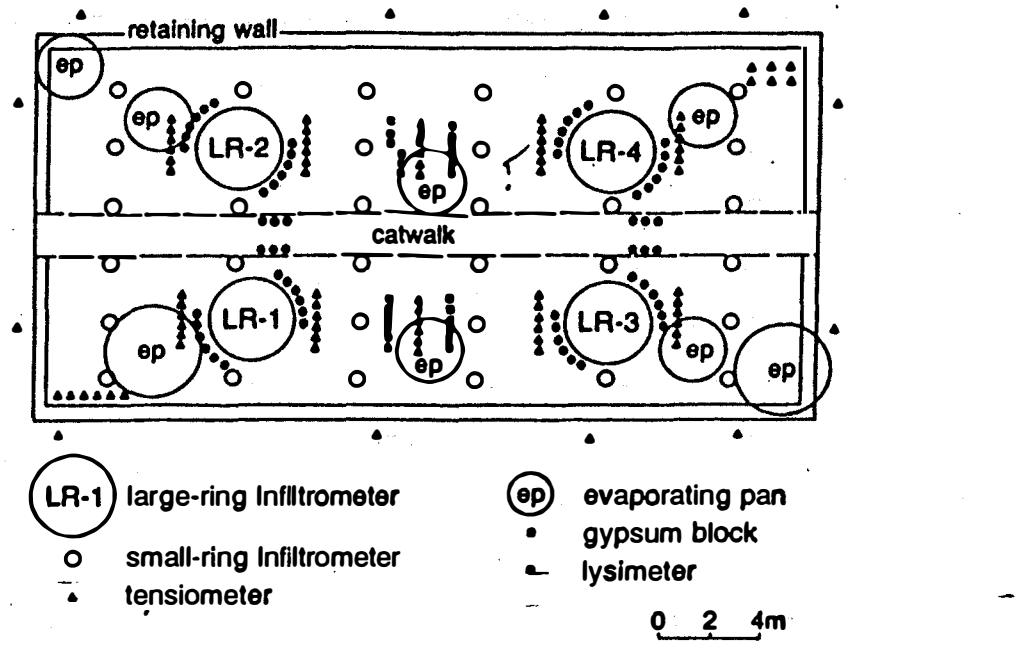

a.

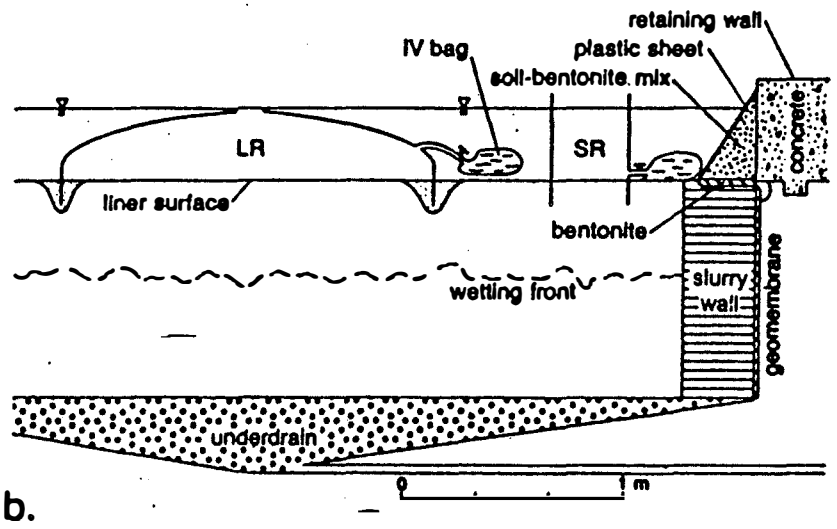

b.

Figure 1. Instrument design of the soil liner: a) aerial view of liner showing distribution of instruments: b) cross section through the retaining wall, and a small ring and a large ring infiltrometer.

Sixty tensiometers were installed in the liner to monitor the movement of moisture and changes in hydraulic head. Ten nests with six tensiometers per nest were installed so that soil tension could be measured at six depths (10, 18, 33, 51, 69, 89 cm) and ten locations in the liner (Fig. 1a). Two years after the liner was flooded, 55 of these tensiometers are operational. Each tensiometer consists of a ceramic porous cup connected with plastic tubing to either a 5 or 15 PSI differential-pressure transducer; the tubing and cup are filled with water. Changes in soil moisture are measured by the transducer as pressure differences in the tensiometer system with respect to atmospheric pressure. The transducers convert the pressure changes to output voltages. The voltages were automatically recorded every 10 minutes, converted to tension (as centimeters of water), and then averaged once daily and stored in a datalogger. A complete description of the tensiometer, installation techniques, and operation can be found in Krapac et al. (1989a).

Tension values were corrected to compensate for the weight of the column of water between the porous cup and the transducer (see Krapac et al., 1989 for details). An additional correction was made to the tension values to account for transducer null offset. Null offset is the value that a differential transducer reports when both measurement ports are open to the atmosphere. In theory, this value should be zero volts; however, in practice, it is usually some non-zero number that is fairly constant and usually less than the equivalent of a tension of 10 cm of water, but sometimes as high as 30 cm of water. Transducers with large null offsets were replaced. Null values were measured for 3 days, while the datalogger continued to record transducer output voltages at 10 minute intervals. The average voltage for the third day was used for the null offset correction for each individual transducer. Barometric pressure and temperature also affected tension values in the liner (Krapac et al., 1989a); however, these effects were minimized by using data collected from periods when "near-normal" barometric pressure prevailed.

Average soil tensions were calculated for all six depths (layers) in the liner for 25 months (i.e., from pre-ponding to 2 years after ponding). A maximum of ten tension values, one at each tensiometer nest, were used to determine the average tension for each of the six sampling depths in the liner. Anomalous tensions caused by instrumental error and malfunctions were not used.

Results

Infiltration Measurements

Water-Balance Method

The water-balance was used to determine the overall infiltration flux into the liner over the two-year period between April 1988 and April 1990. The volume of water lost to evaporation was subtracted from the volume of water added to the pond to maintain a constant level; the resultant volume (5478.8 L) was assumed to have infiltrated into the liner. On the basis of these data, the infiltration flux for the entire liner was estimated to be 8.4×10^{-8} cm/s; however, this estimate is an average of both initial and steady-state infiltrability and does not account for changes with time. Using the cumulative-infiltration volume approach (Fig. 2), a more accurate measure of the "average" infiltration flux into the liner can be obtained. The infiltration flux of the liner, using a least-square regression of the cumulative-infiltration data over the last two years, is 6.4×10^{-8} cm/s ($r^2 = 0.97$). This flux represents the amount of water that had infiltrated into the liner from day one to day 730 after ponding.

An estimate of the depth of the wetting front two years after ponding was calculated based on measurements of bulk density (1.84 g/cm^3) and initial moisture content (0.21 cm^3/cm^3) of the liner, an area of infiltration of 1.3×10^6 cm^2, 5478 L of water having infiltrated into the liner, and assuming a uniform wetting front, a total porosity of 33% with 21% of the pores initially filled with water. The wetting front was calculated to be 44 cm below the liner surface, or approximately half way through the liner after 2 years of ponding. Consequently, the expected time of breakthrough, based on water balance data, is approximately 4 years after ponding (mid-April, 1992).

A three-fold periodic change in infiltration rate for the entire liner was observed in the water balance cumulative-infiltration plot (Fig. 2). During the 2 years of monitoring the liner there was an increase, followed by a decrease and than an increase in infiltration rate which occurred in mid-October, mid-March, and mid-October, respectively. These changes corresponded to the seasons and approximately the time when the liner shelter's heater cycled on in October and off in March and April; this relationship suggests that the infiltration rate fluctuations may be temperature related. For example, Jaynes (1990) observed a cyclical variation in the infiltration rate of ponded soil as a result of diurnal changes in soil temperature.

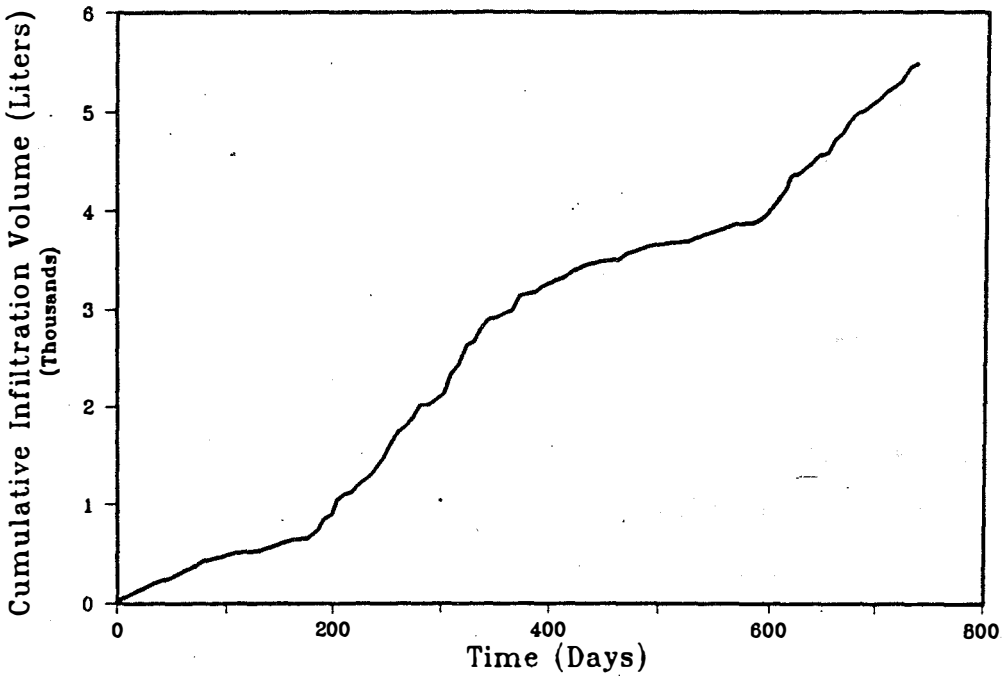

Figure 2. Cumulative infiltration from April 1988 to April 1990 for the entire liner.

Another possible explanation is that the use of the shelter's heater caused errors in evaporation measurements. These relationships, are currently under investigation.

Infiltrometer Method

The infiltration-flux data (representing steady-state infiltrability) for the SR- and LR- infiltrometers form two statistically distinct populations (Fig. 3 a,b). The SR-infiltrometer fluxes (the distribution on the left side of the diagram) were found to be log-normally distributed on the basis of the Kolmogorov-Smirnov test at the 95% confidence level. This type of distribution is consistent with work by Rogowski (1972), Nielson et al. (1973), and Parkin et al. (1988) who reported the lognormal spatial distribution of soil hydraulic properties. The infiltration flux for each LR- and SR-infiltrometers at steady-state infiltrability (between May, 1988 and April, 1990) are listed in Table 1. The mean infiltration flux and variance based on the first and second year monitoring of the liner are summarized in Table 2. The infiltration fluxes for both the LR- and SR-infiltrometers exhibited a small variance suggesting a relatively homogeneous distribution of the infiltration flux over the liner. The LR- and SR-infiltrometers mean infiltration fluxes, calculated from only the second year of monitoring data, differ by approximately one order of magnitude, and are 5.8×10^{-9} and 6.0×10^{-8} cm/s, respectively. The mean infiltration fluxes of the two data sets were found to be statistically different at a 99.9% confidence level, as determined from a t-test.

The reason for the difference between the SR- and LR-infiltrometer fluxes is unclear; however, a possible explanation is leakage of water around or through the grout seal of the LR-infiltrometers. Evidence for this leakage included observations of gas bubbles emanating from the grout-soil interface outside and inside the ring during maintenance operations. The gas bubbles indicate a connection between the inside of the LRs and the liner pond. Excavation of a prototype liner (Albrecht et al., 1989) showed that bonding between the fiberglass of the infiltrometer and the liner material was imperfect suggesting a possible source of the leakage. Although the magnitude of the leakage appeared small, it may be significant compared to the very low infiltration flux. Analyses of water within the LR-infiltrometers revealed that little (if any) tritiated pond water had entered the infiltrometers seven months after the introduction of tritium to the pond.

Preliminary analyses of gas samples collected from the LR-infiltrometers showed a dominance of H_2S and CH_4, and a deficiency of O_2 relative to N_2 suggesting the presence of anaerobic bacteria within the

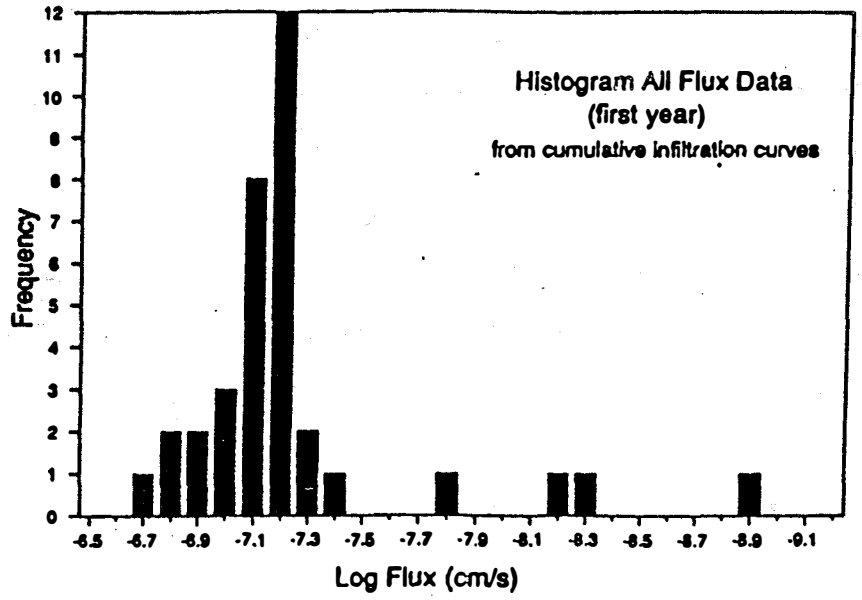

a.

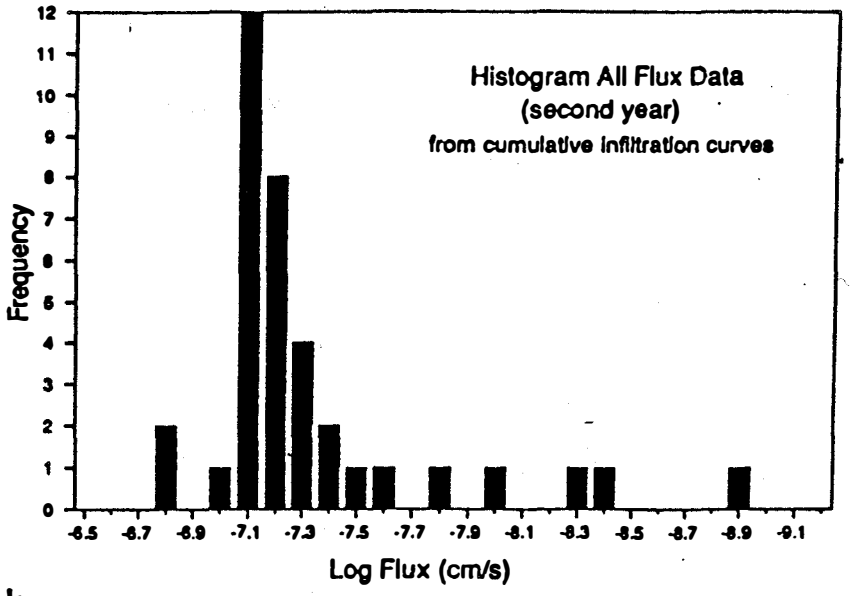

b.

Figure 3. Histograms of log-transformed fluxes measured by the SR- and LR-infiltrometers after: a) one year of infiltration; b) two years of infiltration.

Table 1. Summary of the infiltration fluxes measured by the infiltrometers during the first and second years of monitoring the liner.

Infiltrometer Number	Infiltration Flux (cm/s) 1988 - 1989	Infiltration Flux (cm/s) 1989 - 1990	% Change in Flux[a]
LR-1	1.2×10^{-9}	5.4×10^{-9}	350 I
LR-2	1.5×10^{-8}	1.0×10^{-8}	33 D
LR-3	6.8×10^{-9}	1.6×10^{-8}	135 I
LR-4	5.1×10^{-9}	1.3×10^{-9}	75 D
SR-1	1.3×10^{-7}	6.4×10^{-8}	51 D
SR-2	1.1×10^{-7}	8.9×10^{-8}	19 D
SR-3	1.6×10^{-7}	1.6×10^{-7}	0 NC
SR-4	1.9×10^{-7}	1.5×10^{-7}	21 D
SR-5	7.7×10^{-8}	7.7×10^{-8}	0 NC
SR-6	6.1×10^{-8}	6.9×10^{-8}	13 I
SR-7	6.4×10^{-8}	6.4×10^{-8}	0 NC
SR-8	8.6×10^{-8}	8.6×10^{-8}	0 NC
SR-9	6.3×10^{-8}	3.2×10^{-8}	49 D
SR-10	5.4×10^{-8}	7.7×10^{-8}	43 I
SR-11	6.3×10^{-8}	1.0×10^{-7}	59 I
SR-12	6.4×10^{-8}	6.4×10^{-8}	0 NC
SR-13	6.9×10^{-8}	6.0×10^{-8}	13 D
SR-14	5.9×10^{-8}	5.9×10^{-8}	0 NC
SR-15	8.7×10^{-8}	5.9×10^{-8}	32 D
SR-16	8.3×10^{-8}	3.6×10^{-8}	57 D
SR-17	6.6×10^{-8}	4.0×10^{-8}	39 D
SR-18	8.8×10^{-8}	5.0×10^{-8}	43 D
SR-19	1.0×10^{-7}	7.4×10^{-8}	26 D
SR-20	ND	4.2×10^{-9}	ND
SR-21	6.9×10^{-8}	5.3×10^{-8}	23 D
SR-22	6.4×10^{-8}	4.6×10^{-8}	28 D
SR-23	6.2×10^{-8}	7.4×10^{-8}	19 I
SR-24	7.7×10^{-8}	7.7×10^{-8}	0 NC
SR-25	7.9×10^{-8}	7.9×10^{-8}	0 NC
SR-26	5.1×10^{-8}	5.1×10^{-8}	0 NC
SR-27	8.3×10^{-8}	7.6×10^{-8}	8 D
SR-28	6.6×10^{-8}	6.6×10^{-8}	0 NC
SR-29	1.2×10^{-7}	8.8×10^{-8}	27 D
SR-30	9.3×10^{-8}	7.5×10^{-8}	19 D
SR-31	4.0×10^{-8}	2.5×10^{-8}	38 D
SR-32	1.5×10^{-7}	7.5×10^{-8}	50 D

LR = Large-ring infiltrometers
SR = Small-ring infiltrometers
ND = Not determined

[a] I = Increase in flux
D = Decrease in flux
NC = No change in flux

Table 2. Geometric mean, Log mean, and standard deviation of infiltration fluxes measured by the large-ring and small-ring infiltrometers and the water balance.

Instrument	Infiltration Flux (cm/s)	Log Mean of Infiltration	Standard Deviation*	Sample Size
LR (1st Year)	5.0×10^{-9}	-8.301	0.458	4
LR (2nd Year)	5.8×10^{-9}	-8.237	0.474	4
SR (1st Year)	8.0×10^{-8}	-7.100	0.152	31
SR (2nd Year)	6.0×10^{-8}	-7.218	0.268	32
Water balance	6.4×10^{-8}			1

*The log mean plus or minus 2 times the log standard deviations corresponds to a range of infiltration flux values from 6.1×10^{-10} to 1.6×10^{-7} cm/s.

large rings and beneath the surface of the liner. The presence of bacteria provides a second possible mechanism for the decrease in infiltration flux for the LRs; that is, the growth of anaerobic bacteria within the liner material may be altering the permeability of the liner surface or near-surface within the LRs. Consequently, the lower infiltration fluxes determined from the LR-infiltrometers are suspect.

Perturbations to Infiltration Rates

Barometric Pressure Effect

The similarity between barometric pressure fluctuations and the log mean infiltration flux for the SR- and LR-infiltrometers (Fig. 4 and 5) indicated an inverse relationship between the two variables. That is, as barometric pressure increases, the infiltration flux decreases; this observed relationship is counter to expectations. Increased pressure should increase pressure on the pond surface, thereby increasing infiltration. This latter type of behavior was observed during a day when particularly high barometric pressure was apparently responsible for increased infiltration rates as measured by the infiltrometers. An explanation for the inverse behavior may be found in a comparison of these data with infiltration data collected from "dummy" ring infiltrometers; infiltrometers built to better understand this relationship (see Krapac et al., 1989a for details). The dummy rings were built such that infiltration of water into the liner

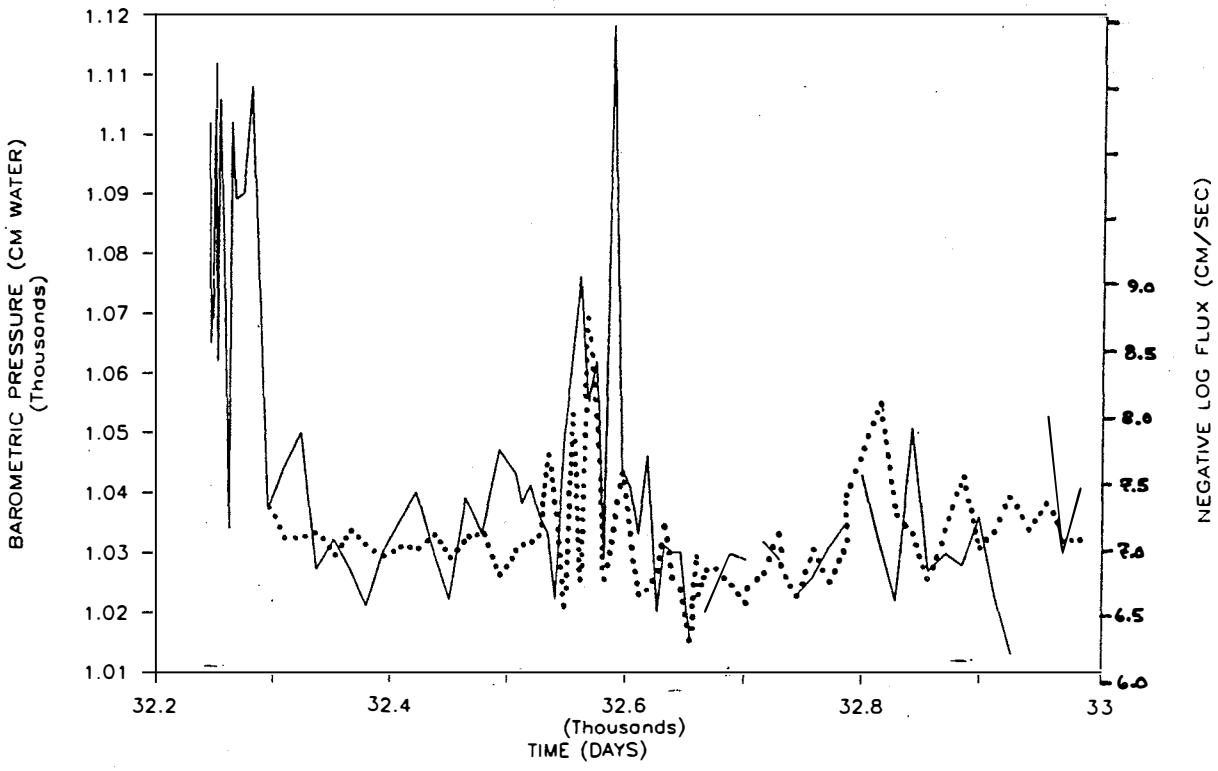

Figure 4. Comparison of SR-infiltrometer fluxes (dots) with barometric pressure (solid line).

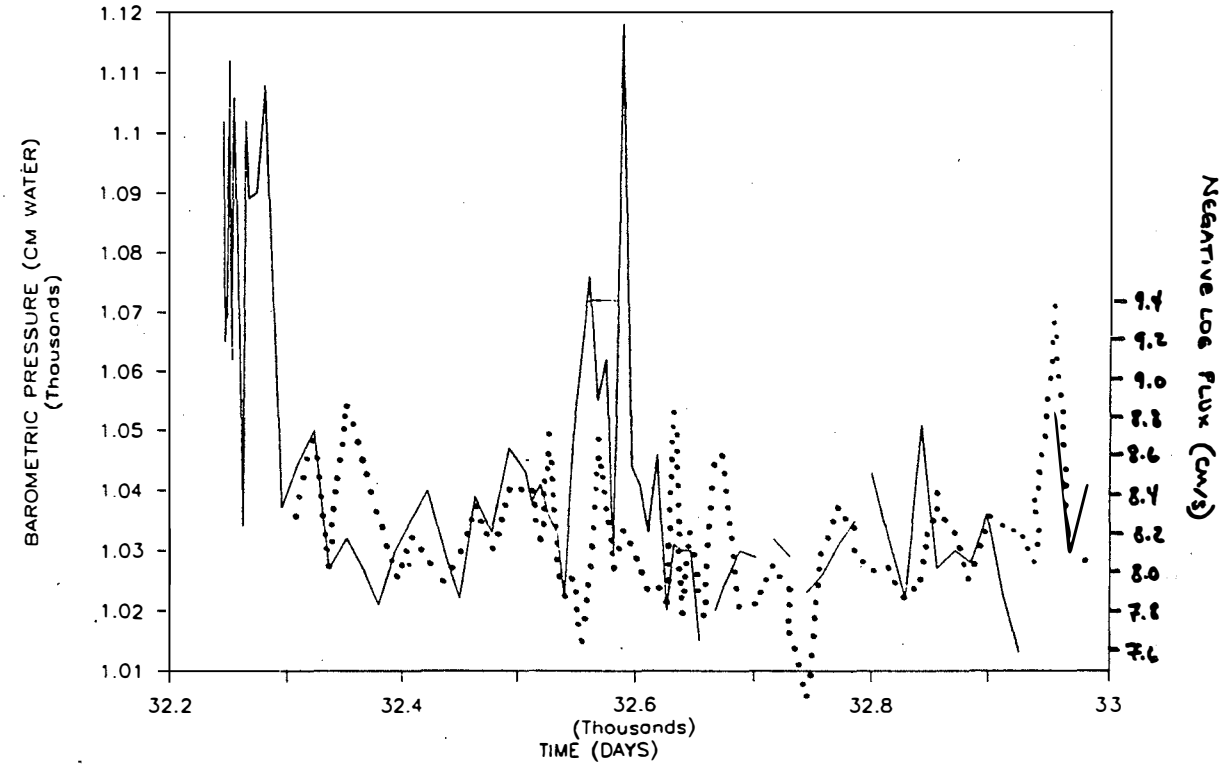

Figure 5. Comparison of LR-infiltrometer fluxes (dots) with barometric pressure (solid line).

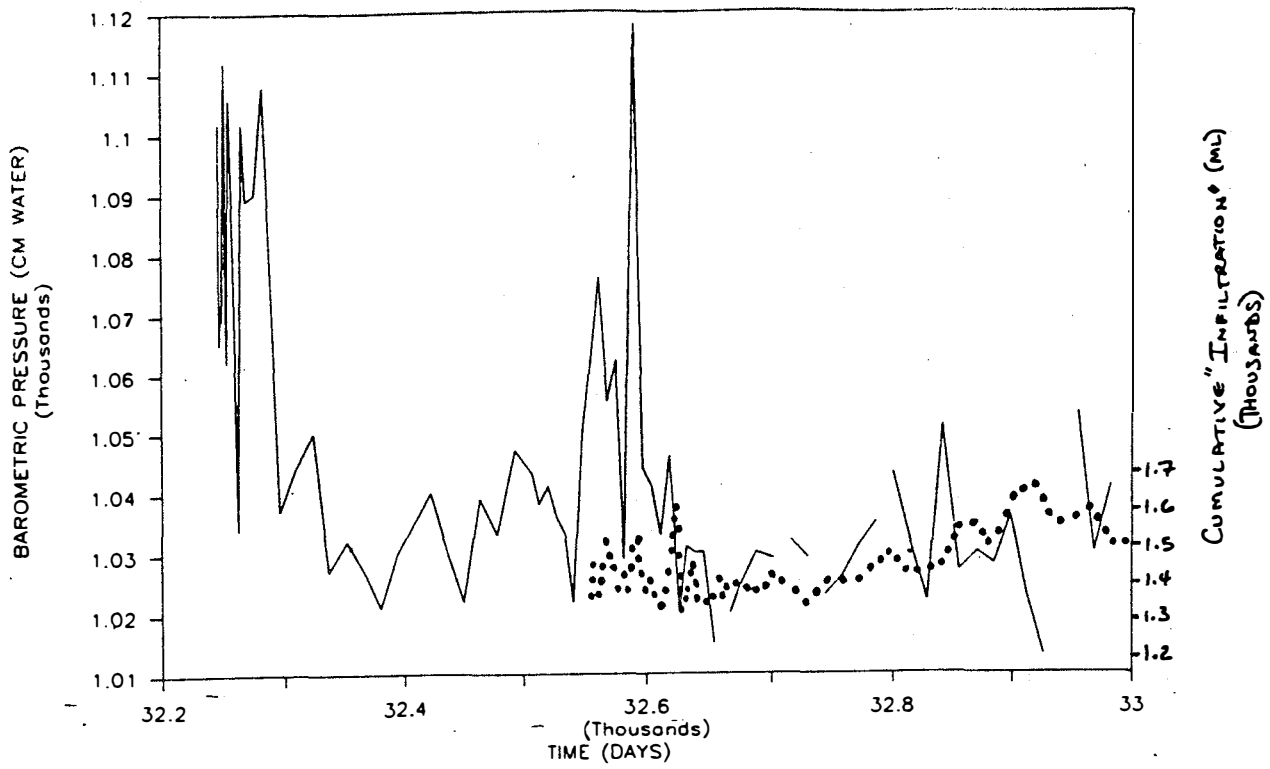

Figure 6. Comparison of dummy ring infiltrometer "cumulative infiltration" (dots) with barometric pressure (solid line).

was eliminated and that apparent infiltration fluxes would be due to measurement error and/or pressure and temperature effects on the instruments. The same trend with barometric pressure was evident in the water loss data from these non-infiltrating rings (Fig. 6). Barometric pressure is apparently affecting water flow into and out of the IV bags attached to all ring infiltrometers. That is, as barometric pressure increases, water is prompted to flow from the ring infiltrometers into the IV bag; conversely, when the barometric pressure is low, water flows from the IV bag back into the ring-infiltrometer. The effect on the IV bags was found to be a transient phenomenon having no effect on long-term measurements (i.e., no net change in volume of water which apparently infiltrated); correction of the data with respect to barometric pressure was considered unnecessary at this level of data analysis. The effect of barometric pressure on the liner is poorly understood, laboratory column studies are underway to verify the effects of barometric pressure and temperature on the infiltration of water into the liner.

Current short term testing of field liners and test pads to determine $K_{(sat)}$ is commonly done using sealed double-ring infiltrometers (SDRI). This technique uses IV bags to measure infiltration volumes. The effect of barometric pressure could bias this type of infiltration data for short-term infiltration experiments.

Pressure induced measurement error could be especially critical for those liners that are marginal in their achievement of the U.S. EPA hydraulic conductivity criterion. As field and laboratory data continue to be collected the significance of the potential measurement errors are being evaluated with respect to compliance regulations.

Construction Effects

During construction of the cutoff wall, installed to retain the pond and ensure one-dimensional flow, stress-release fracturing and localized slumping occurred in the northeast, northwest and southwest corners of the liner (Krapac et al., 1989a). These areas were partially excavated (the entire thickness of the liner was not affected) and recompacted using a 10:1 mixture of soil and bentonite clay. Seven SRs adjacent to these areas (i.e., SR-1, 2, 3, 4, 19, 29, 32) measured a mean infiltration flux during the first year of monitoring of 1.3 X 10^{-7} cm/s, the highest infiltration fluxes of all the SRs, as compared to the other small rings (6.7 X 10^{-8} cm/s). During the second year of monitoring, infiltration fluxes measured by these same infiltrometers decreased. The cause for the decrease in flux is not exactly known but is likely due to the hydration of the bentonite with a corresponding decrease in available soil pore volume and conductivity.

Areal Distribution of Infiltration Fluxes

Geostatistical Analysis of Infiltrometer Data

Geostatistical analysis of the liner infiltration data was used to estimate the mean infiltration flux for the entire liner and for each quadrant of the liner. A structural analysis (Journel and Huijbregts, 1978) was performed to construct and interpret sample variograms, and to select a model variogram to best fit the structure of the log flux data. The variogram is used to obtain an estimate of the covariance structure of the measurements (in this case infiltration flux) at various spatial positions. The variogram is thus able to relate the variance of data collected at various sampling distances. The model variogram was used in the kriging analysis to determine the mean infiltration-flux values.

Geostatisitical analyses were performed with log-transformed infiltration flux data collected during the first year of monitoring from the SR-infiltrometers. The infiltrometers believed to have been affected by cut-

off wall construction and a leaking infiltrometer (SR 20) were not used for these analyses. Subsequent analyses included additional SR-infiltrometer data, as well as data collected during the second year of monitoring the liner.

For the initial analyses, experimental directional variograms (Fig. 7) were calculated in five directions (0, 30, 60, 90, and 120 degrees) with respect to an east-west traverse across the liner using flux measurements for the first year of monitoring from 25 (SR 1, 2, 3, 4, 19, 20, and 32 eliminated from the data set) of the 32 SR-infiltrometers . Only data pairs that fell within 10 degrees of the specified angle were used in the calculations; the lag (distance between data pairs) for the directional variograms was dictated by the instrument spacing. An experimental isotropic variogram was also calculated in which all data pairs, regardless of direction, were used to construct a variogram. The use of directional variograms was limited because of the relatively few data pairs (minimum of 7) at a given lag available for use at the various directions. Figure 7 shows that the 95% confidence interval about the sample variance (based on the chi-square statistic) is large enough to include most of the directional variogram values. This confidence interval was based on the assumption that the log infiltration flux values were independent and uncorrelated. However, the values from closely-spaced infiltrometers were correlated (see next page) and Priestley (1981) has shown that for a one-dimensional correlated random process with an exponential covariance, the confidence interval about the sample variance will be larger than if the samples were autocorrelated. Thus, the confidence interval (Fig. 7) is probably an underestimate of the uncertainty in the variance estimate. Since directional variograms were calculated with few pairs of data points and were within the confidence interval of the sample variance, the directional variograms were assumed to be statistically indistinguishable from the isotropic variogram. The isotropic variogram was used for all subsequent calculations.

Following the calculation of the experimental variogram, a model variogram was fit to the experimental isotropic variogram. The approach used to fit the model variogram, referred to as validation (Journel and Huijbregts, 1978; Englund and Sparks, 1988), involved sequentially removing one data point and using the remaining data points to predict the missing value (via kriging). For each data point, the normalized error, defined as the measured value (infiltration flux) minus the kriged or predicted value divided by the square root of the estimation variance, was calculated. If the model variogram was an

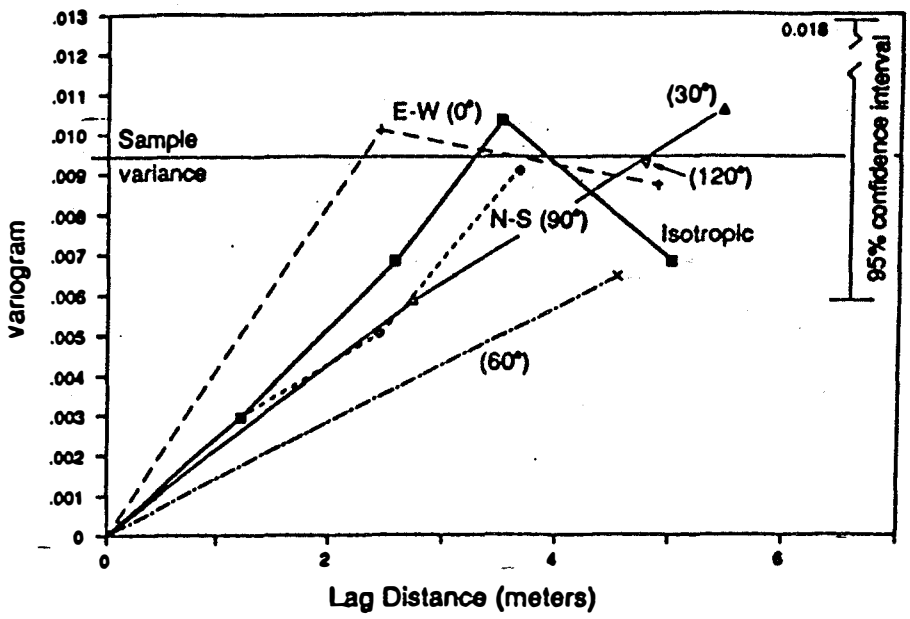

Figure 7. Semi-variogram of log-transformed fluxes measured by the SR-infiltrometers along transects of the liner.

entirely correct representation of the spatial variability, the mean normalized error should have had a value of 0 and a mean squared value of 1. Validation was performed with five possible model variograms and the variogram which most closely produced the mean and mean squared normalized error of 0 and 1 was chosen as the best variogram for use in subsequent kriging estimations. The form and parameters of the five model variograms chosen for validation are given in Table 3. In addition to the validation procedure, the effect of using the various model variograms in estimating (via kriging) the mean infiltration flux of each quadrant of the liner was evaluated (Table 4). The fluxes within each of the quadrants were significantly not different regardless of the model variogram model used. An interesting aspect of the results presented in Table 4 is that the north-east quadrant, which had the fewest data points (recall that four SR-infiltrometers were affected by construction in this quadrant) had the largest variation in estimated mean infiltration and that the south-east quadrant which had the most data points, had the least variation. As one would expect, the more observed values present, the less interpolation performed by the kriging and the more strongly the estimated mean was controlled by the observed values.

Table 3. Model variograms used in the validation analysis.

Model Number	Form	Range (meters)	Sill
1	Exponential	6.0	0.009
2	Exponential	8.0	0.015
3	Gaussian	4.6	0.015
4	Spherical	4.6	0.011
5	Linear	3.0	0.010

Table 4. Kriged estimates of the mean quadrant infiltration fluxes for each of the model variograms.

	Infiltration Flux ($\times 10^{-8}$ cm/s)			
Model Number	North-East Quadrant	South-East Quadrant	North-West Quadrant	South-West Quadrant
1	7.0	6.7	7.0	7.1
2	6.9	6.7	7.0	7.1
3	6.8	6.7	7.0	7.2
4	6.9	6.7	7.0	7.1
5	6.8	6.7	7.1	7.1

This exercise illustrates that the number of data points used in the kriging estimate was more critical in determining a mean infiltration flux than which model variogram was selected as input into the kriging routine.

Based on the validation procedure the best fit model variogram was an exponential model (form 1 in Table 3) which had a sill value approximately equal to the sample variance (a sill value of 0.01) with a range of 6.0 m; the range was defined as the lag distance at which the variogram reaches 95% of its sill value. The correlation scale, that is, the lag distance at which the variogram reached 63% of the sill, was approximately 2.0 m. Those measurements (flux), separated by a distance greater than the correlation scale, were considered uncorrelated. Therefore, only adjacent measurements (SR-infiltrometers) in the north-south direction could be considered correlated. This analysis indicated that the sample grid for the liner (spacing and location of the infiltrometers) was well designed to capture the variability of the infiltration over the surface of the liner. More infiltrometers placed closer together would have produce highly correlated infiltration measurements and each value would not have contributed much new information to the data set; conversely, fewer more widely spaced infiltrometers would have possibly missed a zone of the liner with significantly higher or lower infiltration fluxes than the liner as a whole.

To demonstrate the importance of individual data points in the kriging routine, the quadrant mean and liner mean infiltration were estimated with various data values removed from the data set. Using the first year of monitoring data, kriged infiltration fluxes for 3 cases are presented in Table 5. The first case used the same data set (25 of the 32 SR-infiltrometers) that generated the directional variograms and variogram parameters reported above. The second case removed data collected by SR-infiltrometer 29 in addition to the six infiltrometers removed in case 1. Case 3 retained the data from all of the infiltrometers except SR 20; there was no data for SR 20 during the first year monitoring due to instrument malfunction. Four additional cases are presented using data collected during the second year of liner monitoring. Case 4 used the same 25 of 32 SR infiltrometers as case 1 to compare fluxes between the first and second years of monitoring. Case 5 removed SR 20 as well as infiltrometers SR 3 and 4 which had an unusually low infiltration rate. Case 6 retained SR 20, but did not include SR 3 and SR 4 in the data set. Finally, case 7 included all 32 infiltrometers. For each case, a separate model variogram was determined by a visual fit to the respective sample variogram.

Table 5. Mean infiltration fluxes (cm/s) for each liner quadrant with various data points excluded. Results based on infiltration fluxes measured by the small-ring infiltrometers during the first and second year of monitoring the liner.

	YEAR 1		
Quadrant	Case 1	Case 2	Case 3
NE	6.9×10^{-8}	6.9×10^{-8}	1.0×10^{-7}
SE	6.7×10^{-8}	6.7×10^{-8}	6.7×10^{-8}
NW	7.0×10^{-8}	7.0×10^{-8}	7.3×10^{-8}
SW	7.1×10^{-8}	6.4×10^{-8}	7.6×10^{-8}
LINER	7.0×10^{-8}	6.8×10^{-8}	8.0×10^{-8}

	YEAR 2			
Quadrant	Case 4	Case 5	Case 6	Case 7
NE	7.3×10^{-8}	7.4×10^{-8}	7.4×10^{-8}	8.9×10^{-8}
SE	5.8×10^{-8}	5.8×10^{-8}	5.7×10^{-8}	5.7×10^{-8}
NW	5.4×10^{-8}	5.6×10^{-8}	4.2×10^{-8}	4.2×10^{-8}
SW	5.7×10^{-8}	5.6×10^{-8}	4.2×10^{-8}	6.3×10^{-8}
LINER	5.9×10^{-8}	6.2×10^{-8}	5.7×10^{-8}	6.1×10^{-8}

Case 1 = All SR-Infiltrometers except 1, 2, 3, 4, 19, 20, 32.
Case 2 = All SR-Infiltrometers except 1, 2, 3, 4, 19, 20, 29, 32.
Case 3 = All SR-Infiltrometers except 20.
Case 4 = All SR-Infiltrometers except 1, 2, 3, 4, 19, 20, 32.
Case 5 = All SR-Infiltrometers except 3, 4, 20.
Case 6 = All SR-Infiltrometers except 3, 4.
Case 7 = All SR-Infiltrometers.

Validation was deemed unnecessary on the basis of results in Table 4 in which the form of the variogram model chosen in the kriging routine resulted in insignificant estimates of the mean infiltration fluxes.

The mean quadrant infiltration for each case and for the entire liner are given in Table 5. Case 3 and 7 represent the worst case in estimating the flux for the liner. These cases used all of the infiltrometer data (especially for the first year of monitoring) even though some data was suspect. Comparison of estimated fluxes for the various cases suggested that individual data points can influence both quadrant and entire liner mean infiltration values. These cases eliminated various data points (based on reasonable justification) from the data set and represent the range in infiltration fluxes which could be expected to be measured in the liner. It is important to note that none of the cases estimated a mean infiltration flux which could be used to calculate a mean saturated hydraulic conductivity greater than 10^{-7} cm/s.

Tensiometer Data and Hydraulic Head and Gradient

Tension

Soil tensions were measured at six depths in the liner in order to calculate the hydraulic head and subsequently the hydraulic gradient. The soil tension results are based on data collected on or about the 12th day of each month since ponding of the liner. Tension values were selected from days when the average barometric pressure was between 1022 and 1048 cm of water. This range was typical of pressure values recorded since the liner was flooded (Fig. 8). Monthly tension values are listed in Table 6. Average tension values for all sampling depths (layers) on April 8, 1988 (4 days prior to liner ponding) were positive, indicating that no portion of the liner was saturated prior to ponding. One month after ponding, the upper two layers (0 to 18 cm) were saturated; as indicated by the negative tension values. The liner appeared to become saturated to a depth of 33 cm in November, 1988 as tension values in the 33 cm deep tensiometer became consistently negative. Negative tension values in the lower three layers (51, 69 and 89 cm deep tensiometers) correlate with periods of low barometric pressure and high temperature, both of which can cause a decrease of soil tension (Krapac et al., 1989a).

The average soil tensions with respect to depth in the liner for the period December, 1989 to April, 1990 are shown in Figure 9. The tension values at each depth fluctuated with respect to time due to the effects of atmospheric pressure and temperature. Defining soil saturation as zero tension, the liner appeared to be saturated to a depth between 46 and 52 cm (i.e. the depth at which tension values are zero in Fig. 9) two years after ponding of the liner. Estimates of the wetting front based on the tensiometers and water balance (44 cm) are in good agreement.

Hydraulic Head

The average hydraulic head at each monitoring depth in the liner relative to time are shown in Figure 10. Hydraulic head was obtained by subtracting soil tension from the elevation of the tensiometer, assuming that head is composed of only gravity and matrix potentials. For any month, head decreased with depth because tensions decreased in the liner as would be expected for downward water flow. Head at depths of 10 and 18 cm (T1 and T2 in Fig. 10) has been constant since June 1988 - two months after ponding of the liner. The head at a depth of 10 cm was approximately 200 cm of water corresponding to

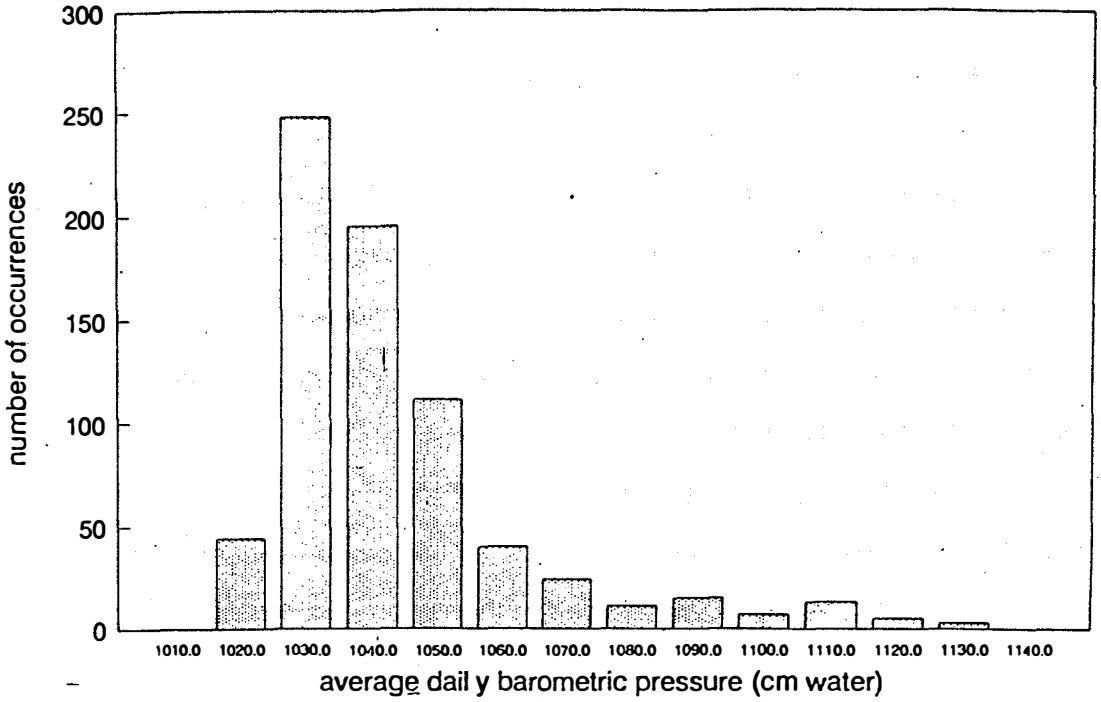

Figure 8. Histogram of barometric pressure recorded at the liner since April 1988. The number below each bar is the maximum value in the range. The bar over 1030 represents all days when barometric pressure was between 1021 and 1030 cm-water.

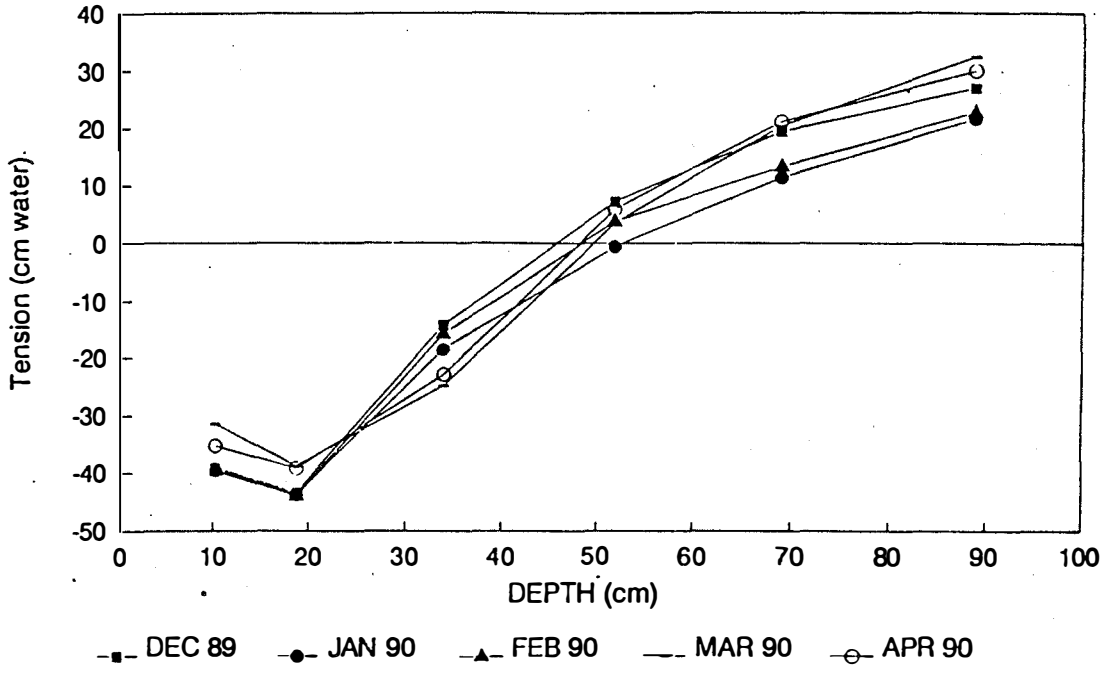

Figure 9. Average tension at various depths in the liner from December, 1989 to April, 1990.

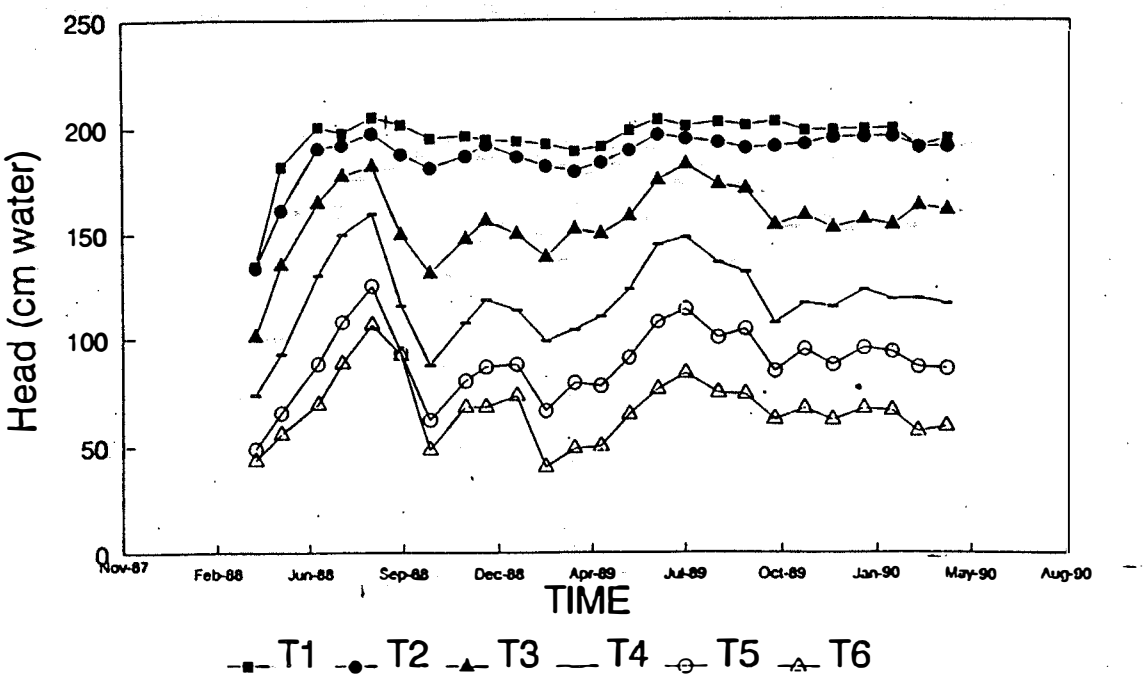

Figure 10. Average head at various depths in the liner from November, 1987 to April, 1990.

the free water head of the pond, indicating that the top 10 cm of the liner was completely saturated. It is unlikely that there can be an increase in head in this layer unless the elevation of the pond was raised. Head in the lower four layers (18 to 91 cm) has fluctuated with changes in barometric pressure and temperature. The effect of pressure and temperature on tension is most pronounced when the soil contains entrapped air (Peck, 1960a and 1960b; Smedema and Zwerman, 1967; Norum and Luthin, 1968; and Turk, 1975). Thus, fluctuations in head indicated that a significant amount of air was and still is entrapped in these layers, even in layer 3 (T3 of Fig. 10) which appeared to be saturated based upon estimated wetting front depths using infiltration data.

Atmospheric pressure and temperature fluctuations and their effects on tension data appeared to be a seasonal phenomena, consequently, a comparison of tension data collected during the same time period but in different years should help to compensate for the observed fluctuations in the tension data. Monthly head values from the first year of data collection were subtracted from the second years' data and the results are presented in Table 7.

Table 6. Average tension values and regression data. Tension values were recorded before the liner was flooded and up to two years after flooding. Regression is for values from 5/06/88 to 4/10/90, time was the independent factor and tension was the dependant factor.

		AVERAGE TENSION (cm-water)					
	Layer designation	T1	T2	T3	T4	T5	T6
	ELV (cm)	160.0	152.2	138.5	122.7	107.1	89.2
Date	Depth (cm)	10	18	33	51	69	89
04/08/88		25.6	18.8	37.4	48.8	58.2	45.9
05/06/88		-21.8	-9.1	3.5	29.9	41.6	33.5
06/15/88		-40.5	-38.3	-26.3	-7.5	18.9	19.7
07/11/88		-37.7	-40.0	-38.8	-27.0	-0.8	1.0
08/11/88		-44.9	-45.4	-43.6	-36.9	-17.9	-17.5
09/11/88		-41.4	-35.3	-11.1	6.8	13.9	-2.9
10/12/88		-35.3	-28.9	7.5	35.1	44.9	40.9
11/18/88		-36.4	-34.7	-8.9	15.1	26.8	21.2
12/10/88		-34.4	-40.1	-17.9	4.3	20.4	21.1
01/11/89		-33.9	-34.3	-11.3	9.1	19.3	15.9
02/11/89		-32.3	-29.6	-0.1	23.7	40.6	49.0
03/14/89		-29.0	-27.1	-13.6	18.4	27.8	40.3
04/11/89		-31.4	-31.6	-11.1	12.3	29.3	39.0
05/11/89		-38.9	-37.5	-19.8	-0.7	16.1	24.5
06/11/89		-44.0	-44.8	-36.8	-21.9	-0.9	13.1
07/11/89		-40.9	-42.7	-44.2	-25.4	-6.9	5.8
08/14/89		-42.8	-41.1	-34.6	-13.2	6.8	14.8
09/11/89		-41.3	-38.4	-32.5	-8.6	2.7	15.4
10/11/89		-43.1	-39.3	-15.7	15.2	22.4	26.9
11/11/89		-38.8	-40.4	-20.3	5.8	12.1	21.7
12/11/89		-39.1	-43.4	-14.2	7.3	19.4	27.0
01/12/90		-39.5	-43.6	-18.4	-0.5	11.5	21.7
02/11/90		-39.6	-43.9	-15.7	3.8	13.3	22.7
03/11/90		-31.4	-38.7	-24.7	3.5	20.4	32.4
04/10/90		-35.3	-39.2	-22.9	5.9	21.1	29.9

Table 7. Comparison of head values recorded during the first and second year of monitoring the liner. A positive value indicates an increase in head, and corresponding increase in soil moisture at that depth.

Depth in liner (cm)	10	18	33	51	69	89
Layer Designation	T1	T2	T3	T4	T5	T6
MAY	17.1	28.4	23.3	30.6	25.5	9.0
JUN	3.5	6.4	10.5	14.4	19.7	6.7
JUL	3.2	2.7	5.4	-1.6	6.2	-4.8
AUG	-2.1	-4.3	-9.0	-23.8	-24.7	-32.3
SEP	-0.1	3.1	21.4	15.5	11.2	-18.3
OCT	7.8	10.4	23.3	19.8	22.5	14.0
NOV	2.4	5.7	11.3	9.3	14.8	-0.4
DEC	4.7	3.3	-3.7	-3.0	1.0	-5.9
JAN	5.6	9.4	7.1	9.6	7.8	-5.8
FEB	7.3	14.3	15.7	19.9	27.3	26.3
MAR	2.4	11.6	11.1	14.9	7.4	7.9
APR	3.8	7.5	11.7	6.4	8.1	9.1
average	4.6	8.2	10.7	9.4	10.6	0.5

A large increase in head was observed between May, 1988 and May,1989 because of the initial flooding of the liner and the initial wetting of the upper layer of the liner. The remainder of Table 7 shows that head values in the upper 5 layers of the liner were generally greater during the second year of monitoring than the first year. From these data, it can be inferred that the upper portion of the liner has had an increase in head as infiltrating water from the pond filled the soil pores. Hydraulic head at the base of the liner appeared to be unchanged, which indicated that no downward-moving water has reached the bottom of the liner .

Hydraulic Gradient

The monthly hydraulic gradient for the entire liner was calculated by regressing the average monthly head values against the average elevation of the tensiometer (Table 8). The gradient is the slope of the regression line, and has had a value of about 2 during the period November, 1989 to April, 1990.

Table 8. Regression analysis on monthly head values. The independent factor was the elevation of the tensiometers located at various depths in the liner, the dependant factor was the average head value for each depth. The slope of the regression line is the overall hydraulic gradient in the liner on that date.

Date	Slope (gradient)	r^2	Date	Slope (gradient)	r^2
04/08/88	1.45	0.96	05/11/89	1.98	0.99
05/06/88	1.88	0.96	06/11/89	1.87	0.99
06/15/88	1.98	0.99	07/11/89	1.73	0.98
07/11/88	1.66	0.98	08/14/89	1.91	0.99
08/11/88	1.46	0.99	09/11/89	1.86	0.99
09/11/88	1.68	0.93	10/11/89	2.11	0.99
10/12/88	2.21	0.95	11/11/89	1.96	0.99
11/18/88	1.97	0.96	12/11/89	2.07	0.98
12/10/88	1.95	0.98	01/12/90	1.97	0.99
01/11/89	1.84	0.97	02/11/90	1.99	0.98
02/11/89	2.26	0.99	03/11/90	2.06	0.99
03/14/89	2.08	0.99	04/10/90	2.07	0.99
04/11/89	2.11	0.99			

Correlation coefficients for this analysis were consistently above 0.90, and commonly at or above 0.98 suggesting a significant relationship between head and depth in the liner.

Hydraulic Conductivity and Transit Time

Hydraulic Conductivity Estimates

The saturated hydraulic conductivity was estimated for the entire liner using measurements of steady-state infiltrability and hydraulic gradient as determined by the infiltrometers and tensiometers, respectively. Darcy's Law for saturated water flow and the Green-Ampt Approximation for infiltration of water into a soil were the two analytical solutions used to calculate the conductivity of the liner. Darcy's Law is written as

$$Q = -K_{sat}IA \qquad [1]$$

where Q is discharge, K_{sat} is saturated hydraulic conductivity, I is the hydraulic gradient, and A is the cross-sectional area of flow. Q/A is the "average" steady-state infiltration flux as measured by the large and small ring infiltrometers and the water balance (Table 2). The gradient measured by the tensiometers at the end of both the first and second year of ponding was 2 (Table 8). The calculated hydraulic

conductivity ranged from 2.5 X 10^{-9} cm/sec to 4.0 X 10^{-8} cm/sec depending on the infiltration data used in the calculation (Table 9).

Green and Ampt (1911) introduced the earliest equation for soil infiltrability which is still widely used. Their method assumes that the wetting front is sharp, the matric potential (tension) at the front is constant, and the wetted zone is uniformly saturated and of constant hydraulic conductivity. This approximation differs from Darcy's Law in that knowledge of the depth of the wetting front is required instead of hydraulic gradient. Under these assumptions, the analytical solution to vertical infiltration is:

$$K = i \left[1 + \frac{h + \psi_f}{L_f}\right]^{-1} \qquad [2]$$

The bracketed term is the hydraulic gradient, h is the ponding depth, ψ_f is the matric potential at the wetting front, L_f is the depth to the wetting front, and i is the steady-state infiltration flux.

The depth of the pond (h) was 29.5 cm for the first 406 days of ponding, and 31.0 cm thereafter; a weighted average of 30.2 cm was used as the pond depth in calculations to determine the hydraulic conductivity from the second year of monitoring data. Tensiometer and water-balance data suggested that the wetting front had moved to an average depth of approximately 35 cm by the end of the first year and to an average depth of approximately 44 cm at the end of the second year. The matric potential at the wetting front was considered the same as that determined by the tensiometers located immediately below the wetting front. Tension values were 7 and 6 cm of water for the first and second years, respectively. Hydraulic conductivity values calculated using the Green and Ampt assumptions are given in Table 9.

Hydraulic conductivity values calculated by the two methods are in close agreement for the first year of monitoring data. The difference between conductivity values between the first and second year infiltration data resulted from the wetting front being deeper after the second year, however neither the gradient nor the tension at the wetting front changed significantly between the first and second year rather than substantial changes in infiltration fluxes. All calculated hydraulic conductivity values are less than 5 X 10^{-8} cm/sec, and are thus a minimum of a factor of two less than the U.S. EPA standard for soil liners.

Table 9. Mean saturated hydraulic conductivity determined from infiltration fluxes using Darcy's Law and Green-Ampt Approximations.

Infiltrometers	Darcy's Law K_{sat} (cm/s)	Green and Ampt K_{sat} (cm/s)
Large Rings first year	2.5×10^{-9}	2.4×10^{-9}
Large Rings second year	2.9×10^{-9}	3.2×10^{-9}
Small Rings first year	4.0×10^{-8}	3.9×10^{-8}
Small Rings second year	3.0×10^{-8}	3.3×10^{-8}
Water Balance	3.2×10^{-8}	3.5×10^{-8}

Tritium Migration Through the Liner

Tritiated water was added to the liner pond on July 20, 1989. The background (pre-tritium) pond concentration was 25.3 disintegration per minute per milliliter (DPM/mL). The initial tritium concentration (Co) was 2334 DPM/mL based on the average of 14 pond samples. The pond concentration had declined to approximately 50% of the initial concentration by April 12, 1990, as tritium diffused into the liner and evaporated from the pond (Fig. 11). Additional tritium was added on May 15, 1990, to raise the pond concentration to 2232 DPM/mL (approximately the initial concentration).

Some soil water samples, regardless of collection depth in the liner, had tritium concentrations above background 30 days after the introduction of tritium to the pond. Figure 12 shows the average tritium concentration profile in the liner at various sampling periods. The tritium concentration has increased with time in the soil pore water to a depth of approximately 33 cm (inflection point).

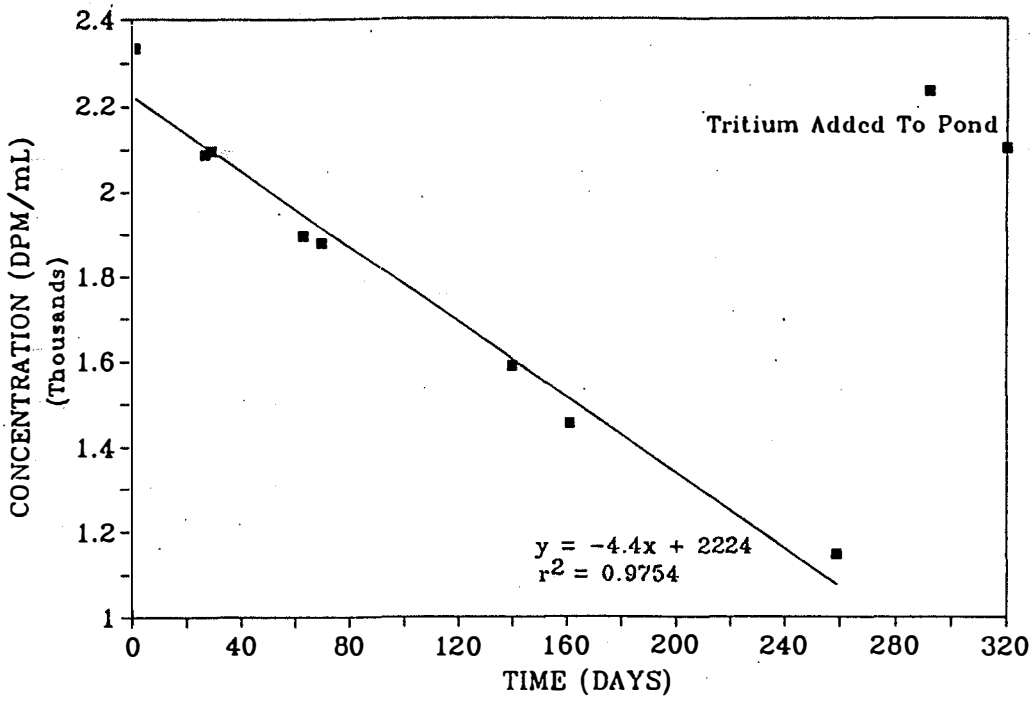

Figure 11. Tritium concentration in pond with respect to time since addition.

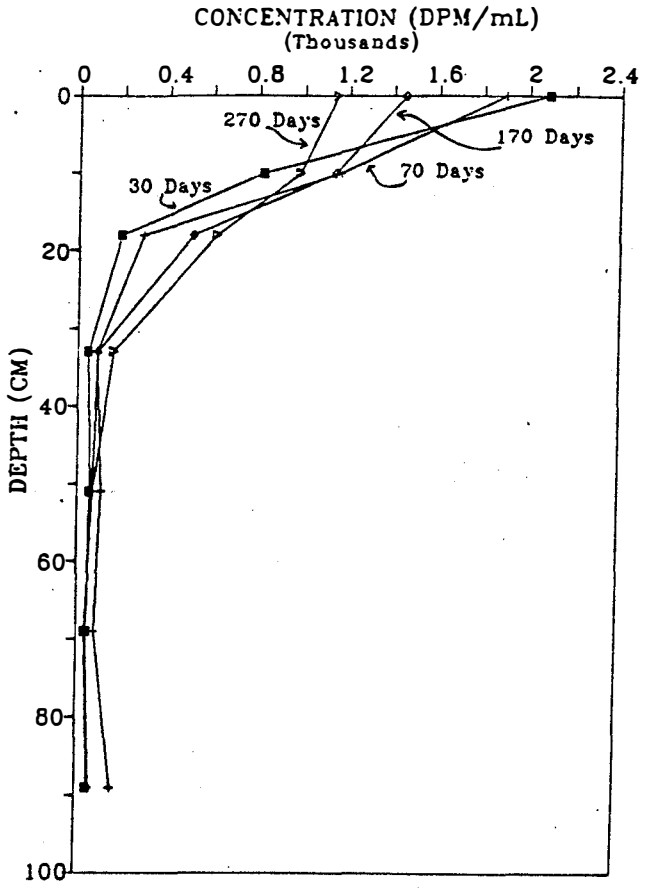

Figure 12. Profile of tritium in the liner at various sampling times since July 20, 1989.

Although the data at the greater depths represents the average of as few as two samples, it appears tritium has migrated throughout the entire liner thickness after 30 days. At depths greater than 33 cm the tritium concentration has remained above background concentrations, but it does not appear to have increased significantly with respect to time since 30 days after the addition of tritium.

The rapid migration of tritium through the liner was not expected. A modeling exercise was undertaken to determine if the observed results could be predicted. CHEMFLO a one-dimensional water and solute model was used to predict tritium movement in the liner. Water movement was modeled using Richards equation. Chemical transport was modeled by means of the convection-dispersion equation. Several CHEMFLO simulations were run in which model parameters such as porosity, advective flow, and concentration were varied to determine the sensitivity of the model to changes in these parameters. Regardless of the parameter values chosen, none of the simulations predicted tritium to migrate in the liner as rapidly as was observed. Figure 13 illustrates the modeled concentration profile using the conditions listed in Table 10. This simulation is presented because it best predicted tritium profiles which matched the observed results; especially at the shallower sampling depths.

The predicted and observed concentration profiles down to 30 cm in Figure 13 are in good agreement for the period of 30 and 70 days after the introduction of tritium; the model was unable to project concentrations above background at depths greater than 30 cm during this time period. However, the predicted 170 and 270 day profiles overestimated the tritium concentration with respect to depth as well as have a "nontypical" concentration distribution in the top 20 cm of the soil profile. The cause for the shape of the distribution profile is apparently an anomaly of the model calculation: further investigation of this feature is being undertaken. The 270 day profile does suggest the soil water tritium concentrations may be above background concentrations to depths of approximately 80 cm.

The model results were not able to predict the observed concentration profiles using the hydrologic parameters that have been measured in the liner (soil tension, hydraulic conductivity, infiltration flux). It appears the model may require calibration with respect to the soil moisture characteristic curve and diffusion coefficient used in the computation of both water and solute movement through the liner.

Table 10. Input parameters for CHEMFLO model.

Bulk density	1.84 g/cc	Dispersion	0
Porosity	0.33	Advective Flow	yes
Saturated Hydraulic Cond.	4×10^{-8} cm/s	Flux at bottom of liner	0
Initial Pressure Potential at Liner Surface	31 cm water	Free Solution Diffusion Coeff.	8.78×10^{-2} cm^2/hr
Initial Pressure Potential at Bottom of Liner	-30 cm water		

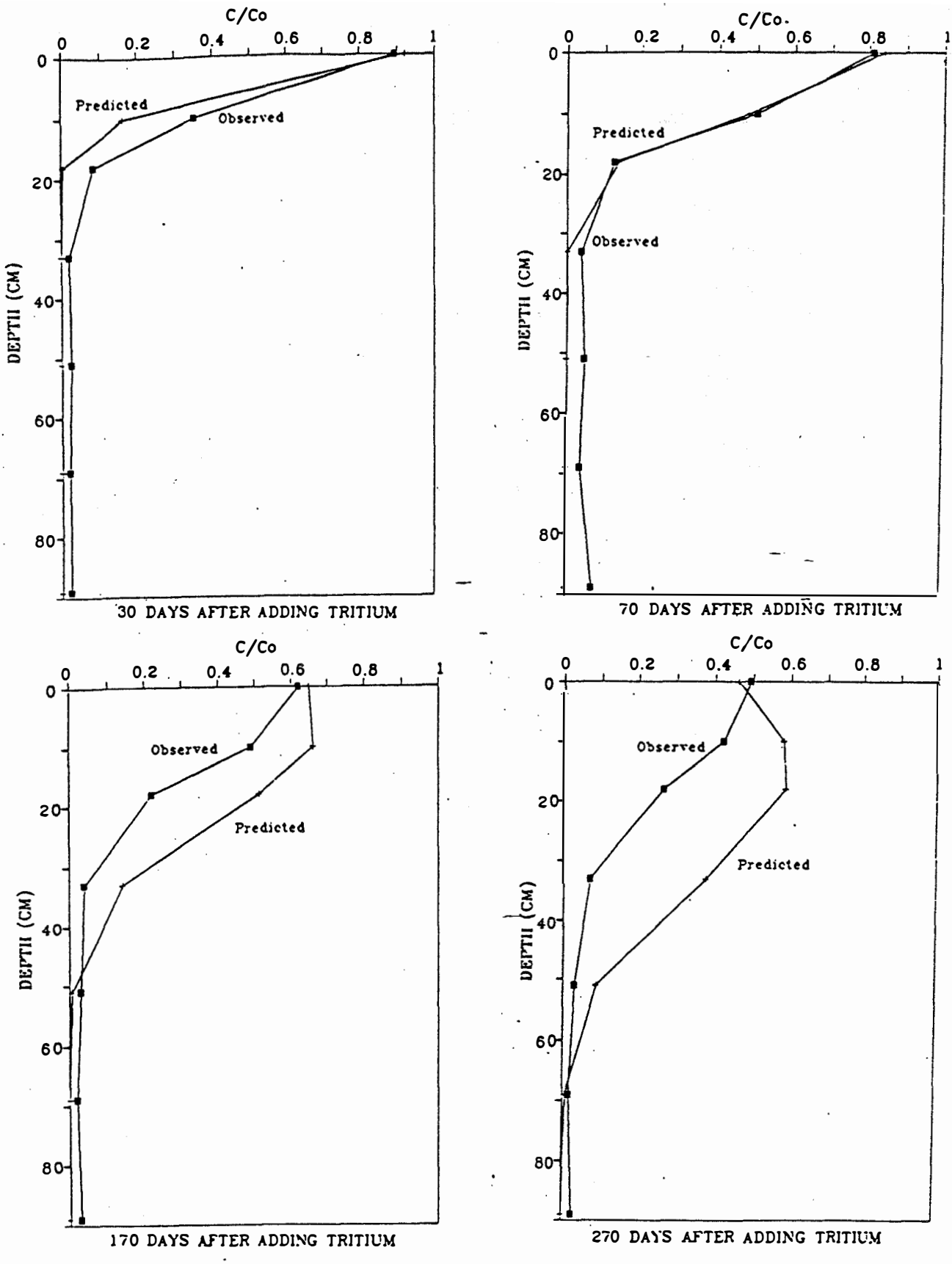

Figure 13. Profiles of tritium concentrations as predicted by the model CHEMFLO and as actually measured in the pore water of the liner.

Summary and Conclusions

A field-scale soil liner, similar to those used in landfills and waste-lagoon facilities, has been monitored for a period of two years to determine: 1) if in situ measurements of saturated hydraulic conductivity could meet the U.S.EPA requirement of $\leq 1.0 \times 10^{-7}$ cm/s, 2) to quantify the aerial variability of the hydraulic properties of the liner, and 3) to determine the transit time for ponded water and tracers through the thickness of the liner. Three scales of monitoring infiltration fluxes have been employed and include a total-pond water-balance approach, large-ring infiltrometers, and small-ring infiltrometers. Soil tensions were determined at various depths in the liner by tensiometers and soil water samples were collected using suction-vacuum lysimeters.

The infiltration fluxes measured by the small-ring infiltrometers were lognormally distributed. The small- and large-ring infiltration fluxes formed two statistically distinct populations. Infiltration fluxes for the large rings were an order of magnitude lower than the infiltration fluxes calculated from the small-ring and water-balance data. Evidence suggests that the large-ring infiltrometers may have experienced either leakage or bacteria-facilitated reduction in permeability during the monitoring period. Cumulative-infiltration curves were found to provide a reliable means of determining the infiltration fluxes for the ring infiltrometers and the water balance. The slope of the curves at steady-state infiltrability provided an "average" long-term infiltration flux of 5.8×10^{-9}, 6.0×10^{-8}, and 6.4×10^{-8} cm/s for the large rings, small rings, and water-balance data, respectively.

Geostatistics were used to evaluate the spatial structure of the infiltration flux variance, and estimated mean infiltration fluxes. The use of several different model variograms did not result in significant differences in estimating infiltration fluxes. Rather the number and sampling location of infiltration data was significant in determining fluxes. The "best-fit" model variogram indicated that the location and spacing of the small-ring infiltrometers was adequate to determine the variability of the infiltration flux over the surface of the liner. Kriged estimates of the mean infiltration fluxes based on the second year of monitoring data for the four quadrants of the liner were similar to one another and range from 4.2×10^{-8} to 8.9×10^{-8} cm/s. The geometric mean of the infiltration fluxes of the entire liner (6.0×10^{-8} cm/s based on the small-ring infiltrometers) is in close agreement with the kriged estimates.

Tension data were affected by barometric pressure and temperature. The tensiometers located at the 10, 18 and 33 cm depths consistently record tension values that were negative after two years of monitoring the liner, indicating saturated conditions. As of spring 1990, the liner was saturated to a depth between 44 and 52 cm. There was evidence of entrapped air below a depth of 20 to 30 cm. Infiltrating water from the pond, and downward flow of water in the liner caused an increase in head throughout most of the liner. Heads at the base of the liner have not increased, indicating that little or no water has yet infiltrated to that layer. The hydraulic gradient remained unchanged between the first and second year of monitoring the liner and was approximately 2 . The upper head value is fixed at about the elevation of the pond; so this gradient value will not decrease until downward-infiltrating water reaches the base of the liner, thereby increasing the hydraulic head in the lower most layer.

The hydraulic conductivity of the liner based on infiltration fluxes measured during the second year of monitoring by the small-ring infiltrometers and the water balance ranged from 3.0 X 10^{-8} cm/s to 4.6 X 10^{-8} cm/s. Conductivities changed by less than a factor of two between the first and second year of monitoring.

Tritium was added to the liner pond in July, 1989. Thirty days after adding tritium, some soil water samples collected at depths as great as 89 cm contained tritium concentrations of approximately twice background. Modeling tritium profiles in the liner was relatively unsuccessful in simulating concentrations approaching those observed at the deeper depths (> 30 cm).

Future Activities

To better understand the response of the soil liner to barometric pressure and temperature fluctuations a laboratory soil column experiment was set up. This experiment will allow temperature and pressure to be varied while monitoring soil tension responses in the column. In addition the effect on water infiltration rates into the soil column will also be monitored.

The observed tritium profile will be used to estimate an effective diffusion coefficient for the liner and efforts will be made to generate a soil moisture characteristic curve in which the soil is being wetted rather than dried during measurements of soil moisture and tension so that hysteresis effects can be eliminated.

Validation of transit time models such as CHEMFLO will continue with emphasis placed on calibration of those model parameters that may not fully represent liner conditions (i.e soil moisture characteristic curve).

References

Albrecht, K.A., B.L. Herzog, L.R. Follmer, I.G. Krapac, R.A. Griffin, and K. Cartwright. 1989. Excavation of an instrumented earthen liner: Inspection of dyed flow paths and soil morphology. Hazardous Waste and Hazardous Materials, v. 5, no. 4, pp. 269-279.

Birks, D. 1989. The garbage route: choosing all the options. World Action for Recycling Materials and Energy from Rubbish (Warmer) Bulletin, v. 23, p. 10.

Daniel, D.E. 1984. Predicting hydraulic conductivity of clay liners. Journal of Geotechnical Engineering, v.110, no. 2, pp. 285-300.

Daniel, D.E. and S.J. Trautwein. 1986. Field permeability test for earthen liners. in S.P. Clemence (ed.), Use of In-Situ Tests in Geotechnical Engineering. American Society of Civil Engineers, New York, pp. 146-160.

Daniel, D.E. and K.W. Brown. 1988. Landfill liners: How well do they work and what is their future? in J.R. Gronow, A.N. Schofield, and R.K. Jain (eds.), Land Disposal of Hazardous Waste: Engineering and Environmental Issues. John Wiley & Sons, New York, pp. 235-244.

Elsbury, B.R., G.A. Sraders, D.C. Anderson, J.A. Rehage, J.O. Sai and D.E. Daniels. 1988. Field and laboratory testing of a compacted soil liner. Draft Final Report to U.S. EPA, Cincinnati, OH. Contract No. 68 03-3250.

Englund, E. and A. Sparks. 1988. GEO-EAS (geostatistical environmental assessment software) user's guide. U.S.EPA, Environmental Monitoring Systems Laboratory, Las Vegas, Nevada, Report EPA/600/4-88/033a.

Green, W.H. and G.A. Ampt. 1911. Studies on soil physics: I. Flow of air and water through soils. Journal of Agricultural Science, v. 4, no. 1, pp. 1-24.

Herzog, B.L. and W.J. Morse. 1986. Hydraulic conductivity at a hazardous waste disposal site: comparison of laboratory and field measured values. Waste Management & Research, v. 4, pp. 177-187.

Hillel, D. 1982. Introduction to soil physics. Academic Press, New York, 364 p.

Jaynes, D.B. 1990. Temperature variations effect on field-measured infiltration. Soil Science Society of America Journal, v. 54, pp. 305-312.

Journel, A.G. and Ch.J. Huijbregts. 1978. Mining geostatistics. Academic Press, 600 p.

Kitanidis, P.K. 1986. Geostatistics in ground water analysis: Applied estimation of spatial functions. in Notes of shortcourse on stochastic and geostatistical analysis in ground water modeling. September 15-19, 1986, International Ground Water Modeling Center, Indianapolis, IN.

Krapac, I. G., Cartwright, K., Albrecht, K., Brutcher, D. F., DuMontelle, P. B., Follmer, L. R., Griffin, R. A., Hensel, B. R., Herzog, B. L., Larson, T. H., Miller, K. W., Panno, S. V., Rehfeldt, K. H., Risatti, J. B., Su, W. 1989a. Field study of transit time through compacted clays. Draft Final Report. U.S. EPA, Cincinnati, Ohio, 241 pp.

Krapac, I.G., S.V. Panno, K.R. Rehfeldt, B.L. Herzog, B.R. Hensel and K. Cartwright. 1989b. Hydraulic properties of an experimental soil liner: Preliminary results. in Proceedings of the 12th Annual Madison Waste Conference, Madison, WI, pp. 395-411.

Nielson, D.R., J.W. Biggar and K.R. Ehr. 1973. Spatial variability in field- measured soil-water properties. Hilgardia, v. 42, pp. 215-259.

Norum, D.I. and J.N. Luthin. 1968. The effect of entrapped air and barometric fluctuations on the drainage of porous mediums. Water Resources Research, v. 4, no. 2, pp. 417-424.

Parkin, T.B., J.J. Meisinger, S.T. Chester, J.L. Starr and J.A. Robinson. 1988. Evaluation of statistical estimation methods for lognormally distributed variables. Soil Science Society of America Journal, v. 52, pp. 323-329.

Peck, A.J. 1960a. The water table as affected by atmospheric pressure. Journal of Geophysical Research, v. 65, no. 8, pp. 2383-2388.

Peck, A.J. 1960b. Change of moisture tension with temperature and air pressure, theoretical. Soil Science, v. 89, no. 6, pp. 303-310.

Priestley, M.B.. 1981. Spectral analysis and time series. Academic Press, San Diego, 890 p.

Rogowski, A.S. 1972. Watershed physics: Soil variability criteria. Water Resources Research, v. 9, pp. 1015-1023.

Rogowski, A.S. 1989. Relationship of laboratory and field determined hydraulic conductivity in compacted layer. U.S. Department of Agriculture Northeast Watershed Research Center, University Park, PA, Draft Final Report of U.S. EPA, Cincinnati, OH.

Rogowski, A.S., B.E. Weinrich and D.E. Simmons. 1985. Permeability assessment in a compacted clay liner. in Proceedings of the Eighth Annual Madison Waste Conference, Madison, WI, pp. 315-337.

Smedma, L.N. and P.J. Zwerman. 1967. Fluctuations of a the phreatic surface, 1. Role of entrapped air under a temperature gradient. Soil Science, v. 103, no.5, pp. 354-359.

Turk, L.J. 1975. Diurnal fluctuations of water tables induced by atmospheric pressure changes. Journal of Hydrology, v. 26, pp. 1-16.

U.S. Environmental Protection Agency. 1988. Design, construction, and evaluation of clay liners for waste management facilities. U.S. EPA Risk Reduction Engineering Laboratory, Cincinnati, OH, EPA/530-SW-86-007F.

U.S. Federal Register, 1987, Hazardous Waste Management Systems: Minimum Technology Requirements. pp B-1 to B-10, April 17, 1987.